

## Twinning in $\text{Pr}_{24}\text{O}_{44}$ : An Investigation by High-Resolution Electron Microscopy

E. SCHWEDA\* AND L. EYRING

*Department of Chemistry and Center for Solid State Science,  
Arizona State University, Tempe, Arizona 85287*

Received March 22, 1988

In the oxidation of  $\text{Pr}_7\text{O}_{12}$  to  $\text{Pr}_{24}\text{O}_{44}$ , the diminished number of defects within the crystal are structurally redistributed. Both structures have a direct relationship to the fluorite lattice for the arrangement of the metal and the oxygen atoms. The defect cluster in these structures consists of two vacancies within the oxygen sublattice that are paired along the [111] direction of the fluorite cell. The transition from one phase to the other is very often accompanied by twinning and also by the formation of antiphase boundaries. It is shown here that twin domains can be related to the loss of symmetry during transformation from the fluorite-related rhombohedral  $\text{Pr}_7\text{O}_{12}$  to the triclinic  $\text{Pr}_{24}\text{O}_{44}$ . The family tree for the rare-earth oxygen-deficient fluorite-related structures is used to explain the twinning observed in  $\text{Pr}_{24}\text{O}_{44}$ . © 1989 Academic Press, Inc.

### Introduction

Increasing attention is being given to relationships in cognate structures. Among the many reasons for this attention is the desire to know the course of chemical reaction in which one member of a family transforms into another. Few of the examples given in the literature have involved composition change in their transformations although this is certainly a valid application of the elegant group theoretical schemes that have been devised (1, 2).

The higher oxides of Ce, Pr, and Tb are structurally related to the fluorite  $\text{CeO}_2$ ,  $\text{PrO}_2$ , and  $\text{TbO}_2$  by an ordered or disordered arrangement of vacant oxygen sites.

\* Present address: Universität Tübingen Institut für Anorganische Chemie, Auf der Morgenstelle 18, D 7400 Tübingen, FRG.

In this study twinning in  $\text{Pr}_{24}\text{O}_{44}$  is used to rationalize the oxidation path followed in its formation from  $\text{Pr}_7\text{O}_{12}$ . Starting with a highly symmetrical structure called the aristotype (3) other related structures can be generated by symmetry reduction and the results represented in the form of a family tree (2).

In the rare-earth oxides of the homologous series  $R_n\text{O}_{2n-2}$  ( $n \leq 4 \leq \infty$ ) the unit cells are known and the space groups have been suggested from X-ray (4), neutron (5, 6), and electron (7) diffraction patterns and from high-resolution electron microscope (HREM) images (8, 9). The space groups suggested are  $R\bar{3}$  for  $R_7\text{O}_{12}$  ( $R = \text{Pr}$  (4),  $\text{Tb}$  (10), and  $\text{Ce}$  (6)),  $P\bar{1}$  for the three compounds  $R_9\text{O}_{16}$  ( $R = \text{Pr}$  (8)),  $R_{11}\text{O}_{20}$  ( $R = \text{Tb}$  (10), and  $\text{Ce}$  (11)), and  $R_{24}\text{O}_{44}$  ( $R = \text{Pr}$  (9)). The structure and space group of  $\text{Pr}_{40}\text{O}_{72}$  ( $n = 10$ ) is less well established.

Phase reactions involving both compositional and structural changes present a valuable opportunity for the application of group theory to transitions among the phases of the homologous series  $\text{Pr}_n\text{O}_{2n-2}$ . A powerful tool for this discussion of structural relationships is sub- and supergroups of the space groups of these phases. In this paper oxidation reactions are to be considered whereas reduction in the  $\text{Pr}_n\text{O}_{2n-2}$  and  $\text{Tb}_n\text{O}_{2n-2}$  systems have already been treated in a related way to some degree (12).

### Symmetry Relationships in the Rare-Earth Oxide System

The group-subgroup relationships in oxidation among the members of the praseodymium oxide system,  $\text{Pr}_n\text{O}_{2n-2}$ , are shown as a family tree in Fig. 1. The family tree delineates the relationships between the anion-deficient structures related to the fluorite sublattice. The formalism used follows that proposed by Bärnighausen (2). In each reaction, arrows show the structural transition according to a maximal subgroup. Using these relationships and the indices of the particular transition one can predict the number and type of orientational twins that are produced in losing point-group symmetry. For example, the index  $t_4$  for the transition  $Fm\bar{3}m$  to  $R\bar{3}m^2$  means that the transformation is classified as translationengleich. The new rhombohedral cell has only one-fourth the volume of the  $Fm\bar{3}m$  cell and only one-fourth of the symmetry elements are kept. The index 4 also indicates quadruple twins are possibly

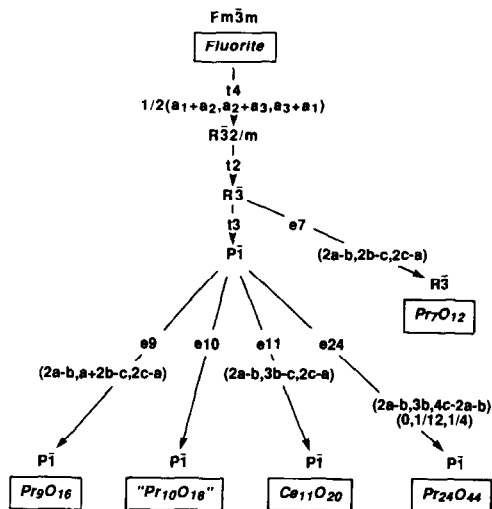


FIG. 1. Symmetry relationships in the praseodymium oxide system.

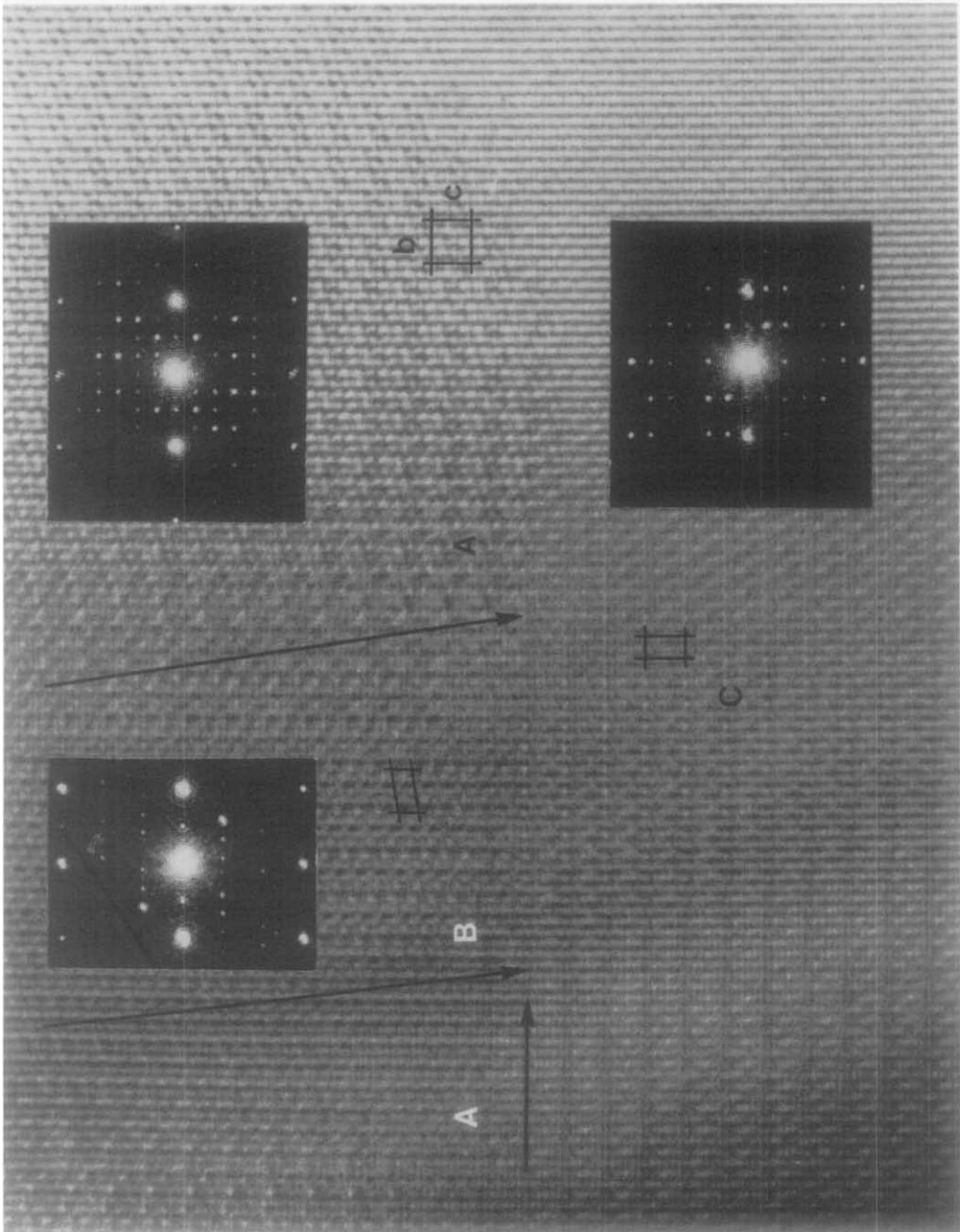
caused by the loss of the fourfold symmetry. An equivalent or isomorphous transition is indicated with an "e" and gives the number of antiphase domains to be expected from this transition.

In this study the  $\text{Pr}_7\text{O}_{12}$  ( $R\bar{3}$ ) was produced by thermal reduction of higher oxides that are fluorite-related.

### Experimental Part

The intermediate  $\beta$  phase  $\text{Pr}_{24}\text{O}_{44}$  was prepared from a 99.999% pure oxide from Research Chemicals, Inc. The starting material, nominally " $\text{Pr}_6\text{O}_{11}$ ," was heated at  $1000^\circ\text{C}$  in a platinum dish for 24 hr in order to remove absorbed  $\text{H}_2\text{O}$  and  $\text{CO}_2$ , cooled to  $200^\circ\text{C}$ , and placed in a desiccator. The

FIG. 2. HREM image of  $\text{Pr}_{24}\text{O}_{44}$ . The cell is shown as a rectangle along the  $[100]$  direction in area A which corresponds to the  $[21\bar{1}]$  direction of the fluorite cell. Area B shows the  $[\bar{1}\bar{1}\bar{1}]_{120}$  rotation twin and area C is the  $[100]_{180}$  rotation twin. Optical diffractograms are inset.



treatment at 1000°C in air produces  $\text{Pr}_7\text{O}_{12}$  which then reoxidizes to  $\text{Pr}_6\text{O}_{11}$  at 200°C. The dry decarbonated product was placed in a quartz tube and annealed at 350 Torr oxygen pressure for 2 days at 400°C to assure an annealed single-phased product with the composition  $\text{Pr}_{24}\text{O}_{44}$ ,  $\beta(1)$ . An X-ray powder diffraction pattern confirmed that the product was the  $\beta(1)$  phase.

A sample of this carefully prepared material was crushed, suspended in ethanol, and applied to a holey carbon film supported on a microscope grid. Electron micrographs were taken with a JEM 4000EX high-resolution electron microscope operated at 400 kV. The images were recorded at optimum defocus using a current density of about 5 A/cm<sup>2</sup>. The thin crystal was oriented along the  $[2\bar{1}\bar{1}]$  fluorite direction which is along the  $a$ -axis of the  $\beta(1)$  cell. Along this shortest axis of the  $\beta(1)$  structure (6.78 Å) the vacancies are aligned parallel to the electron beam. Optical diffraction analysis was used to obtain Fourier transforms of the periodicities present in selected regions of the micrograph.

The image shown in Fig. 2 depicts a triple twin of  $\text{Pr}_{24}\text{O}_{44}$ . By comparing the inserted optical diffraction patterns with those calculated as illustrated in Fig. 3, the twins were identified with respect to their orientation in the fluorite lattice and the twin laws were determined. Area A shows a pro-

jection of  $\text{Pr}_{24}\text{O}_{44}$  along the  $a$ -axis. The projected unit cell along this  $[100]$  direction is marked as a rectangle. The optical diffraction pattern shows this to be identical with one of the 12 independent  $\langle 211 \rangle$  zones of the fluorite structure (Fig. 3). In fact, the whole crystal is oriented along one of the  $\langle 211 \rangle$  zones. This confirms that the fluorite structure itself is only slightly modified and that the f.c.c. cation lattice is maintained throughout the crystal. However, three orientations of the superlattice, which depend on defects in the anion sublattice, are apparent. If the  $a$ -axis in  $\text{Pr}_{24}\text{O}_{44}$  is said to be parallel to the  $[2\bar{1}\bar{1}]$  fluorite direction the twin in area B has an  $a$ -axis parallel to  $[\bar{1}12]$  and in area C an  $a$ -axis parallel to the  $[2\bar{1}\bar{1}]$  fluorite direction. The twin axis between A and B is the fluorite  $[\bar{1}\bar{1}\bar{1}]_{120}$  and the twin axis between A and C is the  $[100]_{180F}$  direction.

The transformation matrices give the relationship between the unit cell of  $\text{Pr}_{24}\text{O}_{44}$  and the fluorite cell for these twins as follows:

$$\begin{pmatrix} a \\ b \\ c \end{pmatrix}_F = 1/2 (M) \begin{pmatrix} a \\ b \\ c \end{pmatrix}_{24}$$

1. The relationship between twins A and B is given by the matrix  $M$ . The twin axis is the fluorite  $[\bar{1}\bar{1}\bar{1}]_{120}$ .

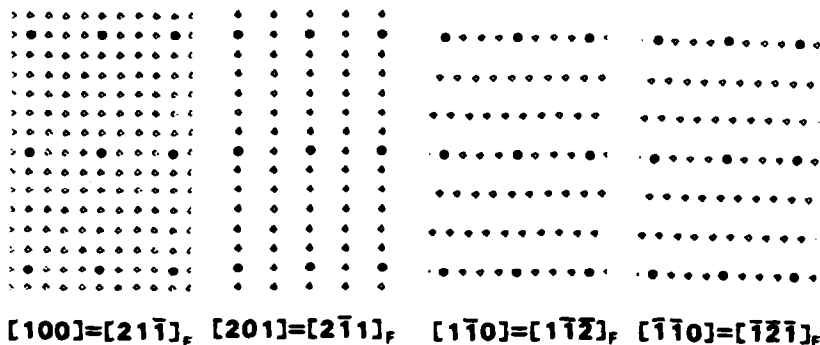
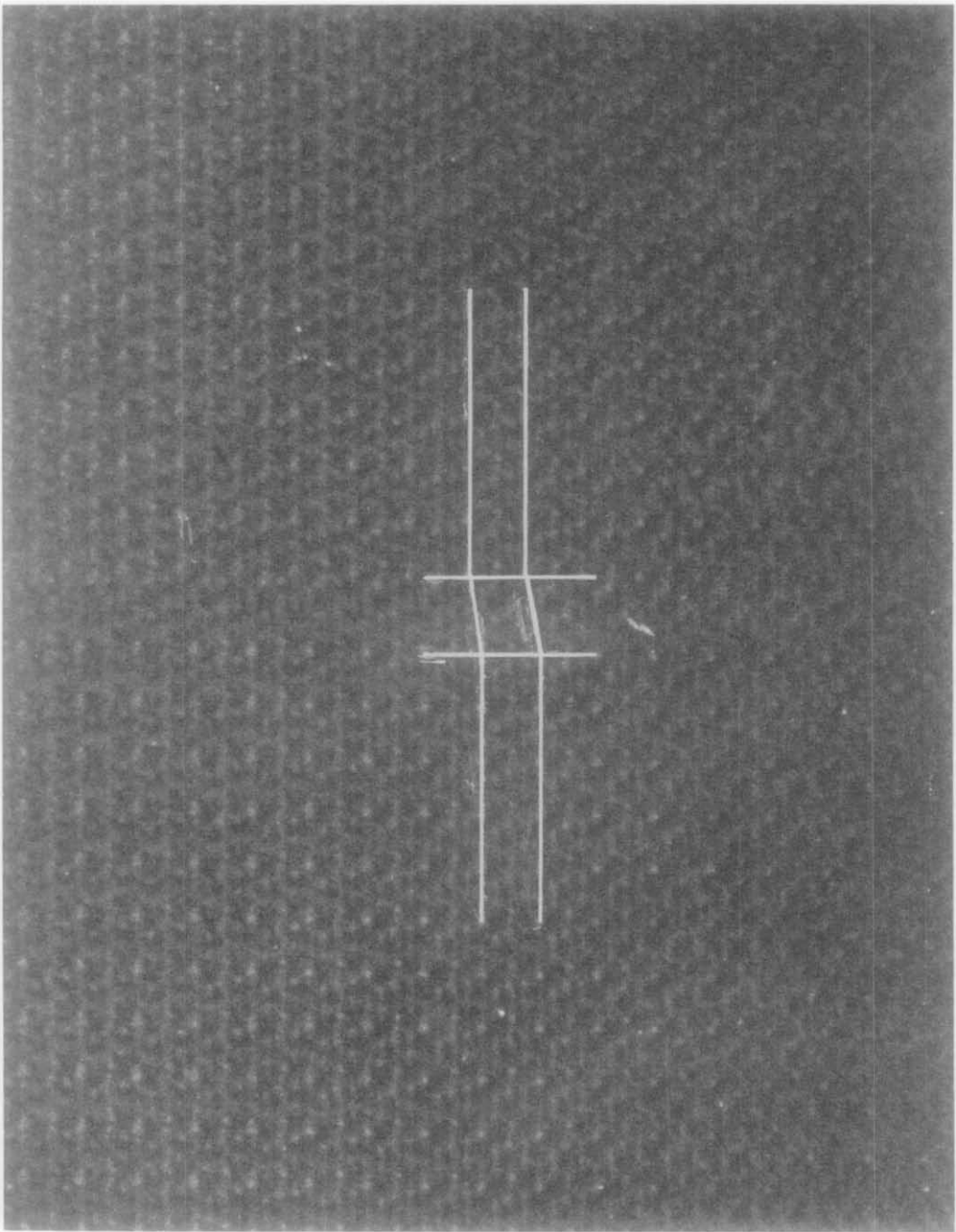


FIG. 3. Calculated diffraction patterns for  $\text{Pr}_{24}\text{O}_{44}$ .

FIG. 4. Antiphase domains in  $\text{Pr}_{24}\text{O}_{44}$ .

$$\begin{pmatrix} 2 & 0 & 2 \\ 1 & 3 & 3 \\ \bar{1} & 3 & 3 \end{pmatrix} \text{---} \begin{pmatrix} \bar{1} & \bar{3} & 3 \\ 1 & 3 & 3 \\ 2 & 0 & 2 \end{pmatrix} \text{---} \begin{pmatrix} \bar{1} & 3 & 3 \\ 2 & 0 & 2 \\ \bar{1} & \bar{3} & 3 \end{pmatrix}$$

2. The relationship between twins A and C is given by the matrix  $M$ . The twin axis is the fluorite  $[100]_{180}$ .

$$\begin{pmatrix} 2 & 0 & 2 \\ 1 & 3 & 3 \\ \bar{1} & 3 & 3 \end{pmatrix} \text{----} \begin{pmatrix} 2 & 0 & 2 \\ \bar{1} & \bar{3} & \bar{3} \\ 1 & \bar{3} & \bar{3} \end{pmatrix}$$

Relating these results to the family tree suggests that during the phase transition from  $\text{Pr}_7\text{O}_{12}$  to  $\text{Pr}_{24}\text{O}_{44}$  the  $[\bar{1}\bar{1}\bar{1}]$  rotation twin is produced by the loss of the threefold axis during the symmetry reduction from  $R\bar{3}$  to  $P\bar{1}$ , and the  $[100]$  rotation twin is produced by the loss of the fourfold axis during symmetry reduction from  $Fm\bar{3}m$  to  $R\bar{3}_m^2$  in the fluorite structure. In Fig. 4 one of the antiphase boundaries predicted by the e24 index in the family tree is presented.

Reduction of  $\text{PrO}_2$  to form the successive intermediate phases  $\text{PrO}_2 \rightarrow \text{Pr}_{24}\text{O}_{44} \rightarrow \text{Pr}_{11}\text{O}_{20} \rightarrow \text{Pr}_{10}\text{O}_{18} \rightarrow \text{Pr}_9\text{O}_{16} \rightarrow \text{Pr}_7\text{O}_{12} \rightarrow \text{Pr}_2\text{O}_3$  is more difficult to relate by group-maximal subgroup considerations. It is known that at least in some cases the transitions occur via a disordered state. For example,  $\text{Tb}_{11}\text{O}_{20}$  or  $\text{Tb}_7\text{O}_{12} \rightarrow \text{TbO}_x$  (disordered)  $\rightarrow \text{Tb}_2\text{O}_3$  (13). It has also been observed that when the higher oxides of Pr or Tb are reduced by electron beam heating, domains of any of the intermediate phases can be observed to nucleate and grow without apparently going through the reduction sequence (14).

## Conclusion

Group theoretical methods are useful tools when used in conjunction with high-resolution electron microscopy in studying systems undergoing phase reactions involving a compositional change. These combined techniques infer the history of a material as well as suggesting the mechanism

of transition. In the interpretation of HREM images the symmetry relationships can explain possible twinning and the formation of antiphase boundaries.

## Acknowledgments

This work was supported by an NSF grant (DMR 8516381). The facilities of the National Center for High Resolution Electron Microscopy (DMR 8306501) within the Center for Solid State Science at Arizona State University were used. The willing and extensive help of Professor D. J. Smith with the JEM 4000EX as well as fruitful discussions with Professor D. J. M. Bevan on the space group of  $\text{Pr}_{24}\text{O}_{44}$  are gratefully acknowledged.

## References

1. H. WONDRAUSCHEK AND W. JEITSCHKO, *Acta Crystallogr. Sect. A* **32**, 664 (1976).
2. H. BÄRNIGHAUSEN, *Match* **9**, 139 (1980).
3. H. D. MEGAW, "Crystal Structures: A Working Approach," Saunders, Philadelphia (1973).
4. N. C. BAENZIGER, H. A. EICK, H. S. SCHULDT, AND L. EYRING, *J. Amer. Chem. Soc.* **83**, 2219 (1961).
5. R. B. VON DREELE, L. EYRING, A. L. BOWMAN, AND J. L. YARNELL, *Acta Crystallogr. Sect. B* **31**, 971 (1975).
6. S. P. RAY AND D. E. COX, *J. Solid State Chem.* **15**, 33 (1975).
7. P. KUNZMANN AND L. EYRING, *J. Solid State Chem.* **14**, 229 (1975).
8. E. SUMMERVILLE, R. T. TUENGE, AND L. EYRING, *J. Solid State Chem.* **24**, 21 (1978).
9. E. SCHWEDA AND L. EYRING, submitted for publication.
10. R. T. TUENGE AND L. EYRING, *J. Solid State Chem.* **41**, 75 (1982).
11. P. KNAPPE AND L. EYRING, *J. Solid State Chem.* **58**, 312 (1985).
12. C. BOULESTEIX AND L. EYRING, *J. Solid State Chem.* **66**, 125 (1987).
13. C. BOULESTEIX AND L. EYRING, *J. Solid State Chem.* **71**, 458 (1987).
14. L. EYRING, *High Temp. Science* **20**, 183 (1985).